

Fractional topological phase in one-dimensional flatbands with nontrivial topology

Huaiming Guo¹, Shun-Qing Shen² and Shiping Feng³

¹*Department of Physics, Beihang University, Beijing, 100191, China*

²*Department of Physics, The University of Hong Kong, Pokfulam Road, Hong Kong and*

³*Department of Physics, Beijing Normal University, Beijing, 100875, China*

We show the existence of the fractional topological phase (FTP) in a one-dimensional interacting fermion model using exact diagonalization, in which the non-interacting part has flatbands with nontrivial topology. In the presence of the nearest-neighbouring interaction V_1 , the FTP at filling factor $\nu = 1/3$ appears. It is characterized by the three-fold degeneracy and the quantized total Berry phase of the ground-states. The FTP is destroyed by a next-nearest-neighbouring interaction V_2 and the phase diagrams in the (V_1, V_2) plane is determined. We also present a physical picture of the phase and discuss its existence in the nearly flatband. Within the picture, we argue that the FTP at other filling factors can be generated by introducing proper interactions. The present study contributes to a systematic understanding of the FTPs and can be realized in cold-atom experiments.

I. INTRODUCTION

The discovery of integer (IQHE) and fractional (FQHE) quantum Hall effects opened a window to explore the mystery in condensed matter physics¹⁻³. They are new topological states of quantum matter, which go beyond the Landau's theory of spontaneous symmetry breaking⁴. The studies of these effects enrich our understanding of quantum phases and quantum phase transitions. In his seminal paper⁵, Haldane showed that IQHE can be realized on a lattice model without a net magnetic field. Most recent generalization of the Haldane model to electrons with spin 1/2 gives birth to the time-reversal invariant Z_2 topological insulator (TI), which becomes the current research focus in condensed matter physics due to their many exotic properties⁶⁻¹⁰.

Inspired by this, similar ideas arise for the situation of FQHE and many studies are devoted to realize the fractional topological phase (FTP) on lattice models in the absence of external magnetic fields. Up to now great development has been achieved. Models that exhibit nearly flatband with a nonzero Chern number are proposed in different systems and numerical calculations confirm its existence when interactions are included¹¹⁻²⁰. To gain some insight of FTP, in this paper we focus on the one-dimensional (1D) case. Using exact diagonalization, we calculate the low-energy spectrum and Berry phase of the lowest energy states of a 1D interacting topological flat band model, and identify the FTP at the filling factor, *i.e.*, the average number of electron per site, $\nu = 1/3$. We also present a physical picture of the phase and discuss its possible existence of fractional charges in the nearly flatband. The FTPs at other filling factors can be generated by introducing proper interactions.

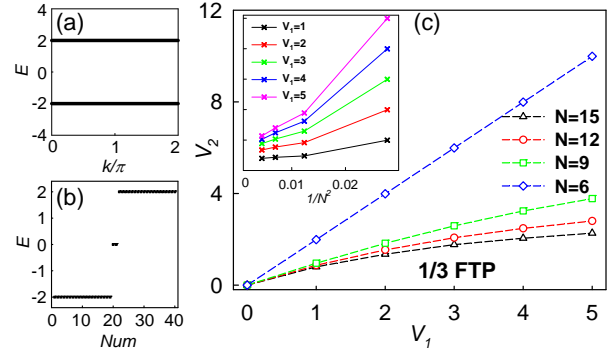


FIG. 1: (Color online) (a) The tight-binding band structure when the parameters satisfy $-M/2 = B = A$, where the bands are flat. (b) Edge modes in the flatband case on a chain of length $N = 20$ with open boundary condition. (c) The phase diagram in the (V_1, V_2) plane at $\nu = 1/3$ for different sizes. The inset shows the size dependence of the critical value V_{2c} at different V_1 . Here $A = B = 1$ and $M = -2$ (in the following calculations if not mentioned, we use these parameters).

II. 1D TOPOLOGICAL FLATBAND MODEL

Consider the 1D non-interacting tight-binding model²¹,

$$H_0 = \sum_i (M + 2B) \Psi_i^\dagger \sigma_z \Psi_i - \sum_{i, \hat{x}} B \Psi_i^\dagger \sigma_z \Psi_{i+\hat{x}} - \sum_{i, \hat{x}} \text{sgn}(\hat{x}) iA \Psi_i^\dagger \sigma_x \Psi_{i+\hat{x}} \quad (1)$$

where σ_x and σ_z are Pauli matrices, and the spinor $\Psi_i = (c_i, d_i)^T$ with c_i (d_i) electron annihilating operator at the site \mathbf{r}_i , which can be obtained by mapping the Dirac equation into a lattice²². In the momentum space Eq.(1) becomes $H_0 = \sum_k \Psi_k^\dagger \mathcal{H}(k) \Psi_k$ with $\Psi_k = (c_k, d_k)^T$ the Fourier partner of Ψ_i and

$$\mathcal{H}(k) = [M + 2B - 2B \cos(k)] \sigma_z + 2A \sin(k) \sigma_x.$$

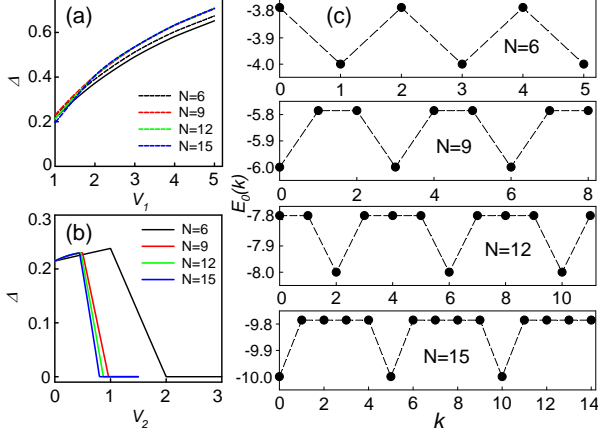


FIG. 2: (Color online) (a) The gap between the ground-states and the excited states versus V_1 at $V_2 = 0$ (solid line) and $V_2 = 0.5$ (dashed line). (b) the gap versus V_2 at $V_1 = 1$. (c) The ground-state energy of each momentum sector at $V_1 = 1$ and $V_2 = 0$ on systems with different sizes.

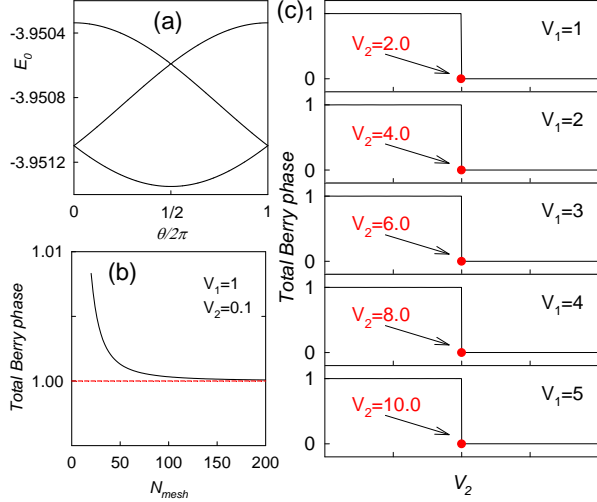


FIG. 3: (Color online) (a) The energies of the ground-states versus θ at $V_1 = 1$ and $V_2 = 0$. (b) The total Berry phase versus the number of divided meshes N_{mesh} . (c) The total Berry phase versus V_2 at different fixed V_1 . Here the parameters are $A = B = 1$ and $M = -1.99$ when the band slightly departs the exact flatness.

The spectrum of $\mathcal{H}(k)$ consists of two bands,

$$E_k^{(1,2)} = \pm \sqrt{[M + 2B - 2B \cos(k)]^2 + [2A \sin(k)]^2}.$$

Usually the two bands are dispersive, but when the parameters satisfy $-M/2 = B = A$, the bands are flat, when $E_k = \pm|2A|$. Also the resulting flatband has non-trivial Berry phase, $\pi \bmod(2\pi)$, which is manifested by the existence of the zero energy modes at the two ends of the system. Thus we realize the topological flatband in one dimension.

III. THE EFFECT OF INTERACTION

Next we study the effect of interactions in the topological flatband. We firstly add nearest-neighbouring (NN) and next-nearest-neighbouring (NNN) interactions to Eq.(1), which are written as,

$$H_I = V_1 \sum_{\langle i,j \rangle} n_i n_j + V_2 \sum_{\langle\langle i,j \rangle\rangle} n_i n_j$$

where $n_i = c_i^\dagger c_i + d_i^\dagger d_i$ is the total number of electrons on site \mathbf{r}_i and V_1, V_2 are the strength of the interactions. We perform the exact diagonalization study of the total Hamiltonian $H_0 + H_I$ on a finite chain of N sites with periodic boundary condition. We denote the number of particles as N_p and the filling factor of the topological flatband is $\nu = N_p/N$. We have carried out the calculations at $\nu = 1/3$, and identified the FTP in which the ground-states are three-fold degenerate. We firstly glance at the phase diagram in the (V_1, V_2) plane, which is shown is Fig.1 (c). By turning on V_1 , the ground-state is three-fold degenerate and the FTP emerges. The ground-state is separated from higher eigenstates by a finite gap Δ . As shown in Fig.2 (a), the value of the gap increases with the strength of V_1 , indicating that the FTP is more stable at larger V_1 . After turning on V_2 , the value of the gap vanishes and the FTP is destroyed at a critical value V_{2c} [see Fig.2 (b)], which marks the boundary of the FTP in the phase diagram. We determine the boundaries of the FTP on different sizes of the chain and find that the region of the FTP is shrunk as the size increases. However according to the results on the sizes we can access, it is reasonable to deduce that the FTP exists in the thermodynamic limit.

The system under consideration has translational symmetry and the momentum of the eigenstate is a good quantum number. Thus the Hamiltonian can be diagonalized in each sector with the momentum $q = 2\pi k/N$ ($k = 0, 1, \dots, N-1$), which allows us to examine the character of the low-energy spectrum in the momentum space. In Fig.2 (c) we show the ground-state energy of each momentum sector at $V_1 = 1$ and $V_2 = 0$ on systems with different sizes. It has been shown that for these parameters the ground-states are three-fold degenerate. Here we further demonstrate that the three states are in different momentum sectors. If k_1 is the momentum sector for one of the ground-state manifold, the other states should be obtained in the sectors $k_1 + N_p$ and $k_1 + 2N_p$ (module N). For the cases with nonzero V_2 the results are similar. The gap between the ground-states and the excited-states is clearly demonstrated in Fig.2 (c). And we find that the value of the gap is independent of the size of the system for $V_2 = 0$ [the solid line in Fig.2 (a)], while for $V_2 \neq 0$ it is dependent [the dashed line in Fig.2 (a)].

To further confirm the existence of the FTP, we study the topological property of the ground-states. It can be understood in terms of the total Berry phase of the

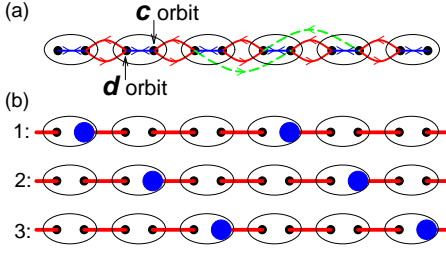


FIG. 4: (Color online) (a) The schematic representation of the resulting Hamiltonian after rotating the Pauli matrices. The hopping amplitudes of the blue, red and green bonds are $M + 2B$, $-(B + A)$ and $-(B - A)$ respectively. (b) The three degenerate ground-states at $\nu = 1/3$.

ground-states. By using the twisted boundary conditions, it is expressed as^{23,24}

$$\gamma = \sum_{j=1}^3 \oint i \langle \psi_{\theta}^j | \frac{d}{d\theta} | \psi_{\theta}^j \rangle,$$

where θ is the twisted boundary phase which takes values from 0 to 2π and ψ_{θ}^j are the corresponding many-body wave functions of the three-fold degenerate ground-states. Since the flatband has nontrivial topology, the total Berry phase of the ground-states is expected to be $\text{mod}(\gamma, 2\pi) = \pi$. Each ground state shares the Berry phase $\pi/3$ averagely. When the bands are exactly flat, the energy of the ground-states remains the same as θ varies. So to perform the calculations, we adjust the parameter M a little and make the band nearly flat. As shown in Fig.3 (a), the ground-state energies are slightly split and vary with θ . Then we calculate the total Berry phase at different V_1 on a chain with $N = 6$ and show the result in Fig.3 (c). It shows that the total Berry phase gets nontrivial value π for small V_2 and jumps to zero as V_2 is further increased. The obtained critical values V_{2c} are in good consistence with those from the energy spectra. Moreover for other lattice sizes, the results are the same. In the calculations, we divide the range of the boundary phase $[0, 2\pi]$ into $N_{mesh} = 100$ meshes, which allows the results in an acceptable precision. With the above methods, we also identify the FTP at $\nu = 1/4$.

IV. MAPPING TO THE SU-SCHRIEFFER-HEEGER MODEL

The Hamiltonian described by Eq.(1) can be obtained through a dimensional reduction from the Bernevig-Hughes-Zhang model which describes the two-dimensional topological insulator HgTe²⁵. Performing a cyclic permutation of the Pauli matrices $\sigma_z \rightarrow \sigma_x$, $\sigma_x \rightarrow \sigma_y$, and $\sigma_y \rightarrow \sigma_z$ in Eq. (1), the Hamiltonian becomes,

$$H'_0 = \sum_i (M + 2B)(c_i^\dagger d_i + d_i^\dagger c_i) \quad (2)$$

$$- \sum_{i,\hat{x}} ([B + \text{sgn}(\hat{x})A]c_i^\dagger d_{i+\hat{x}} + [B - \text{sgn}(\hat{x})A]d_i^\dagger c_{i+\hat{x}}),$$

where the hopping amplitudes are all real. If the two orbits on each site are viewed as two separate sites, it describes the free electrons on a chain with NN and next-next-nearest-neighbouring hoppings, as shown in Fig.4(a). In the flatband case of $A = B = -M/2$, it can be simplified as,

$$H'_{0,flat} = -2A \left(\sum_i c_i^\dagger d_{i+1} + d_{i+1}^\dagger c_i \right),$$

which is the Su-Schrieffer-Heeger model in the limit case where only NN hopping exists and every other bond is broken completely^{26,27}. The model is solvable by setting $\gamma_{i,\pm} = (c_i \pm d_{i+1})/\sqrt{2}$. Then $H'_{0,flat} = -2A(\sum_i \gamma_{i,+}^\dagger \gamma_{i,+} - \gamma_{i,-}^\dagger \gamma_{i,-})$ and then we have the two flatband spectra as shown in Fig.1(a). At $\nu = 1/3$, the lowest energy state is highly degenerate. In the presence of the NN interaction in Eq. (1), there are three configurations of the ground states where the NN interaction between the electrons can be minimized, $|g_\alpha\rangle = \Pi_n \gamma_{3n+\alpha,+}^\dagger |0\rangle$ with $\alpha = 0, 1, 2$. These three states $|g_\alpha\rangle$ are the charge-density-wave as depicted in Fig. 4(b), which breaks the translational symmetry. However, we found that the lowest energy states in each momentum sector K has a uniform density distribution of electron, which is in consistence with the translational symmetry in Eq.(1). The states are the linear combination of the three degenerate states $|g_\alpha\rangle$. Utilizing the lattice translational operator, we can construct the three states as eigenstates of the momentum $K : |g, K\rangle = \frac{1}{\sqrt{3}} \sum_\alpha e^{i\alpha K} |g_\alpha\rangle$ where $K = 2n\pi/3$ ($n = 0, 1, 2$). Thus these three states are those in the presence of interactions. It can be checked as a limit of the nearly flatband, in which the density distribution of electron is always uniform. Therefore the ground-states show three-fold degeneracy. After the NNN interaction is turned on, though the electrons begin to interact with each other, the three configurations still have the same lowest energies for small V_2 and the three-fold degenerate ground-states persist for $V_2 < V_{2c}$. In particular with the above picture n -fold (n other than three or four) degenerate ground-states can be generated by introducing proper interactions.

V. THE FTP IN THE NEARLY FLATBAND

Up to now we have established the existence of the FTP in topological flatband. It is natural to ask whether the phase persists in the nearly flatband. In the following we let the band dispersing by tuning the parameter M and study the properties of the ground-states. As shown in Fig.5 (a), when $\delta M = 2 - M \neq 0$ the the energy of three lowest energy states are split. An energy gap Δ_1 appears between the lower two-fold degenerate states and the upper one, whose value increases

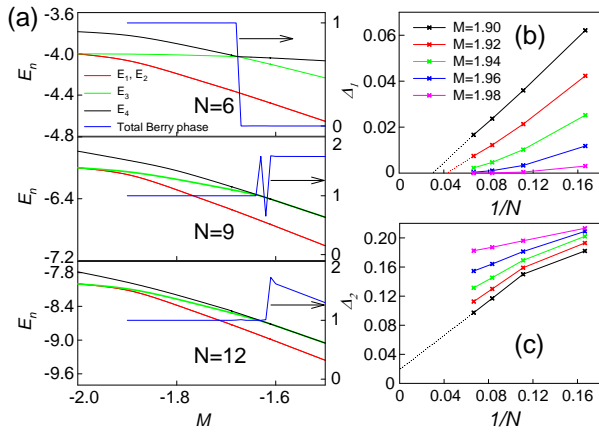


FIG. 5: (Color online) (a) The energies of the lowest four states and the total Berry phase of the lowest three states versus M . (b) and (c) the finite-size analysis of Δ_1 and Δ_2 respectively. Here $\nu = 1/3$.

with δM . Meanwhile the energy gap Δ_2 separating the three lowest energy states from the fourth lowest energy state decreases with δM and vanishes at a critical value δM_c . Moreover beyond δM_c the total Berry phase of the three states with the lowest energies is no longer quantized to π , which implies the occurrence of a topological quantum phase transition. Now the question becomes whether the three lowest states are still degenerate for $0 < \delta M < \delta M_c$ in the thermodynamic limit. To this end, the finite-size analysis of two energy gaps Δ_1 and Δ_2 at several small δM is presented in Figs. 5(b) and (c). The results demonstrate that Δ_1 tends to vanish while Δ_2 survives in the thermodynamic limit, i.e., for a large N limit. So the splitting of the degeneracy of the lowest energy states may be due to the finite-size effect and the FTP persists in the nearly flatband.

VI. CONCLUSIONS

We have studied the FTP in a 1D interacting topological flatband model using exact diagonalization. By introducing the NN and NNN interactions, we identify the FTP at $\nu = 1/3$, in which the ground-states are three-fold degenerate. Moreover the degenerate ground-states are in different momentum sectors and are equally spaced with the interval of N_p . With the above method, we have obtained the phase diagram at $\nu = 1/3$ in the (V_1, V_2) plane. We also study the total Berry phase of the low-energy states and find that it gets a quantized value π when the system is in the FTP. The phase boundary from the total Berry phase is in good consistence with that from the low-energy spectrum.

Existence of the 1D FTP is closely related to the underlying physics in dimerized polyacetylene^{25–27}. One explicit consequence of the 1D FTP is the charge fractionalization of the quasi-particles or excitations. Follow-

ing Kivelson and Schrieffer²⁸, in the 3-fold degenerate ground-states, the domain walls or solitons possess the fractional charges of $e/3$, which can be changed by an integer by adding electrons or holes. In our case, suppose a domain wall is formed between two of the three degenerate ground-states. The domain wall can move freely on the chain. When we move the particle one unit, the domain wall moves three units. Since the change in electric dipole moment can be calculated in two equivalent ways, i.e., through the particle motion $e(+1)$ and through the domain wall motion $Q(+3)$, we have $Q = e/3$, which is the fractional excitation associated with the domain wall of the 1D FTP. For strongly interacting systems, it can be also understood very well from the bosonization and the theory of macroscopic polarization by calculating the Berry phases²⁹.

Now we can have a systematic understanding of the FTPs on lattices without net magnetic field in all three dimensions. For the 1D case, the flatband has a non-trivial Berry phase and the excitations with fractional charges characterize the FTP. For the 2D case, the FTP is found in interacting electrons of flatband with a non-trivial Chern number. Its feature is an almost multi-fold degenerate incompressible ground-states with fractional Hall conductance, which is similar to FQHE. Also by combining the two decoupled FTPs formed by spin up and down electrons, we have fractional quantum spin Hall effect or fractional TI with time-reversal symmetry. For the 3D case in nearly flatband characterized by a nontrivial Z_2 topological index and in the presence of repulsive interactions, a 3D fractional TI can be generated. Thus FTP can be realized in interacting electrons with topologically non-trivial bands. The common features are the multi-fold degeneracy of the ground states and topological invariants of all degenerated ground states.

Due to the rapid development of the field of cold atoms³⁰, it is very hopeful to realize the 1D FTP on state-dependent optical lattice with laser-assisted tunneling between adjacent sites^{31–33}. To simulate our Hamiltonian, atoms with four internal states $c_{1,2}$ and $d_{1,2}$ are required, such as ^6Li et al.. Then in the state-dependent optical lattice, atoms in states c_1 and d_1 are at positions $\mathbf{r}_1 = 2n$ and atoms in states c_2 and d_2 are at positions $\mathbf{r}_2 = 2n + 1$, where the lattice constant is $\lambda/4$ with λ the wavelength of the laser generating the optical lattice. We can choose the optical potential large enough to prohibit direct tunneling between neighboring sites. The hoppings in the model are induced by additional lasers driving Raman transitions between different states. By setting different resonance frequencies for different kind of hopping, the non-interacting Hamiltonian can be realized using proper additional lasers. Since the separation between neighboring sites is half the original lattice constant, significant NN interactions can be generated. Also due to the fact that on-site interactions don't affect the FTP, it is very possible to realize the FTP in this scheme. Finally it would be exciting to find real materials exhibiting the FTP.

VII. ACKNOWLEDGEMENTS

The authors would like to thank Z.-C. Gu, Hua Jiang, D. N. Sheng, Jun-Ren Shi and Yi-Fei Wang for helpful discussions. HG is supported by FOK YING TUNG EDUCATION FOUNDATION and NSFC under Grant

No. 11104189; SS is supported by the Research Grant Council of Hong Kong under Grant No. N_HKU748/10; SF is supported by the Ministry of Science and Technology of China under Grant Nos. 2011CB921700 and 2012CB821403, and NSFC under Grant No. 11074023.

-
- ¹ K. v. Klitzing, G. Dorda, and M. Pepper, Phys. Rev. Lett. **45**, 494 (1980).
 - ² D. C. Tsui, H. L. Stormer, and A. C. Gossard, Phys. Rev. Lett. **48**, 1559 (1982).
 - ³ R. B. Laughlin, Phys. Rev. Lett. **50**, 1395 (1983).
 - ⁴ L. D. Landau and E. M. Lifschitz, Statistical Physics (Pergamon, London, 1958).
 - ⁵ F. D. M. Haldane, Phys. Rev. Lett. **61**, 2015 (1988).
 - ⁶ C. L. Kane and E. J. Mele, Phys. Rev. Lett. **95**, 226801 (2005).
 - ⁷ C. L. Kane and E. J. Mele, Phys. Rev. Lett. **95**, 146802 (2005).
 - ⁸ J. E. Moore, Nature **464**, 194 (2010).
 - ⁹ M. Z. Hasan and C. L. Kane, Rev. Mod. Phys. **82**, 3045 (2010).
 - ¹⁰ X. L. Qi and S. C. Zhang, Rev. Mod. Phys. **83**, 1057 (2011).
 - ¹¹ E. Tang, J. W. Mei and X. G. Wen, Phys. Rev. Lett. **106**, 236802 (2011).
 - ¹² T. Neupert, L. Santos, C. Chamon, and C. Mudry, Phys. Rev. Lett. **106**, 236804 (2011).
 - ¹³ K. Sun, Z. Gu, H. Katsura, and S. Das Sarma, Phys. Rev. Lett. **106**, 236803 (2011).
 - ¹⁴ F. Wang and Y. Ran, Phys. Rev. B **84**, 241103 (2011).
 - ¹⁵ X. Hu, M. Kargarian, and G. A. Fiete, Phys. Rev. B **84**, 155116 (2011).
 - ¹⁶ T. Neupert, L. Santos, S. Ryu, C. Chamon, and C. Mudry, Phys. Rev. B **84**, 165107 (2011).
 - ¹⁷ C. Weeks and M. Franz, Phys. Rev. B **85**, 041104 (2012).
 - ¹⁸ X. L. Qi, Phys. Rev. Lett. **107**, 126803 (2011).
 - ¹⁹ D. N. Sheng, Z. C. Gu, Kai Sun, L. Sheng, Nature Communications **2**, 389 (2011).
 - ²⁰ Y. F. Wang, Z. C. Gu, C. D. Gong, and D. N. Sheng, Phys. Rev. Lett. **107**, 146803 (2011).
 - ²¹ H.-M. Guo and S. Q. Shen, Phys. Rev. B **84**, 195107 (2011).
 - ²² S. Q. Shen, W. Y. Shan and H. Z. Lu, SPIN **1**, 33 (2011).
 - ²³ R. Resta, Rev. Mod. Phys. **66**, 899 (1994).
 - ²⁴ Q. Niu, D. J. Thouless, and Y.-S. Wu, Phys. Rev. B **31**, 3372 (1985).
 - ²⁵ B. A. Bernevig, T. L. Hughes and S. C. Zhang, Science **314** 1757 (2006).
 - ²⁶ W. P. Su, J. R. Schrieffer, and A. J. Heeger, Phys. Rev. Lett. **42**, 1698 (1979).
 - ²⁷ A. J. Heeger, S. Kivelson, J. R. Schrieffer and W.-P. Su, Rev. Mod. Phys. **60**, 781 (1988).
 - ²⁸ S. Kivelson and J. R. Schrieffer, Phys. Rev. B **25**, 6447 (1982).
 - ²⁹ A. A. Aligia and C. D. Batista, Phys. Rev. B **71**, 125110 (2005).
 - ³⁰ I. Bloch, J. Dalibard, and W. Zwerger, Rev. Mod. Phys. **80**, 885 (2008).
 - ³¹ N. Goldman, D. F. Urban, and D. Bercioux, Phys. Rev. A **83**, 063601 (2011).
 - ³² D. Jaksch and P. Zoller, New J. Phys. **5**, 56 (2003).
 - ³³ F. Gerbier and J. Dalibard, New J. Phys. **12**, 033007 (2010).